Modulation of Base Specific Mutation and Recombination Rates Enables Functional Adaptation within the Context of the Genetic Code

Taison Tan[1], Leonard D. Bogarad[2], Michael W. Deem[1]

[1]Department of Bioengineering and Department of Physics & Astronomy
Rice University
Houston, TX 77005–1892

[2]Division of Biology
California Institute of Technology
Pasadena, CA 91125

February 9, 2008

Corresponding author: Michael W. Deem, Rice University, 6100 Main Street—MS 142, Houston, TX 77005-1892, 713-348-5852, 713-348-5811 (fax), mwdeem@rice.edu.

Key Words:
Codon Usage — Codon Mutation Matrix — Mutation Rate — Recombination Rate

ABSTRACT

The persistence of life requires populations to adapt at a rate commensurate with the dynamics of their environment. Successful populations that inhabit highly variable environments have evolved mechanisms to increase the likelihood of successful adaptation. We introduce a 64×64 matrix to quantify base-specific mutation potential, analyzing four different replicative systems, error-prone PCR, mouse antibodies, a nematode, and *Drosophila*. Mutational tendencies are correlated with the structural evolution of proteins. In systems under strong selective pressure, mutational biases are shown to favor the adaptive search of space, either by base mutation or by recombination. Such adaptability is discussed within the context of the genetic code at the levels of replication and codon usage.

1 Introduction

Viable mutations can potentiate the emergence of new life forms and the adaptation of living organisms to new environmental constraints. Evolution occurs through a hierarchy of genetic events, including base substitution, homologous recombination, insertions, deletions, rearrangements, transpositions, and horizontal transfers (Lawrence, 1997; Pennisi, 1998). Systems such as the adaptive immune system use somatic hypermutation to rapidly search protein space to combat infectious agents. Likewise, error-prone PCR is used in molecular evolution protocols to search space in order to optimize protein function. In addition, pathogens and cancers have evolved effective dynamic mechanisms, often predicated on base substitution, to evade immune and therapeutic selection. In HIV, for example, the high rate of viral mutation makes the development of a vaccine difficult and results in the rapid onset of resistance to many current drugs. Indeed, there is a correspondence between the ability of HIV to evolve drug resistance, the drug regimen given, and the genetic makeup of the strains present in a patient (Lathrop and Pazzani, 1999). Crucial to a thorough understanding of the base substitution process is a mathematically precise quantification of the various mutation rates.

The mutational machinery of hypermutation and recombination is under environment-dependent regulation (Bull *et al.*, 2001). Studies have shown that regulation is possible both in the process of replication and error correction (Sutton and Walker, 2001) and in the type of polymerases expressed (Friedberg *et al.*, 2000; Storb, 2001). The mechanism for maintenance of adaptability traits is population-based and requires a dynamic environment. That evolvability is a group selectable trait has been shown in simulations of digital organisms (Travis and Travis, 2002; Peper, 2003; Ofria *et al.*, 1999; Thearling and Ray, 1997; Wagner and Altenberg, 1996; Altenberg, 1994). Many of the biochemical events necessary to modify adaptability are known. At the simplest level, mutation of a single amino acid site in the *Taq* Pol I enzyme is sufficient to greatly modulate the accuracy of DNA replication (Patel *et al.*, 2001).

The goal of this paper is to show how species can use evolution in populations as a space searching advantage in the context of the genetic code. Base-to-base rates of synonymous, conservative, and non-conservative mutation tendencies for each codon are described, thus allowing for the quantification of evolutionary potential. Base-specific mutation rates are dependent upon the fidelity of the replication machinery, flanking sequences, and other environmental conditions. The base substitution rate is non-uniform because transitions are typically greatly favored over transversions, and purines are typically substituted at a greater frequency than pyrimidines. However, different replication systems have different base specific mutation probabilities. It is here argued that within the context of genetic code, the emergence of replication variants that modulate not only the

overall rate but also base-specific mutation rates allows populations to increase the probability of searching productive survival space under dynamic environmental constraints. Our theory complements previous observations for the immune system (Kepler, 1997), recent observations of codon bias toward increased adaptability in Influenza A (Plotkin and Doshoff, 2003), and recent work on digital organisms showing how adaptability evolves within a population (Travis and Travis, 2002; Peper, 2003; Ofria *et al.*, 1999; Thearling and Ray, 1997; Wagner and Altenberg, 1996; Altenberg, 1994).

A codon mutation matrix that defines in a precise manner the probability per round of a codon mutating by base substitution into another codon is introduced. This matrix provides the rates of all possible 64×64 mutations. From these detailed rates, properties of the codons themselves can be calculated. For example, the codon mutation matrix allows the classification of codons according to their synonymous, conservative, or non-conservative mutabilities. Codons that tend to mutate in a more dramatic, non-conservative fashion are characterized as having a higher evolutionary potential, allowing for a more rapid short-term adaptation.

To describe mutabilities of codons, there currently exists the K_{S} and K_{A} notation (Li *et al.*, 1985). The parameter K_{S} describes the number of synonymous substitutions per site, and K_{A} describes the number of non-synonymous substitution per site. Because of its average character, and because it is based upon sequences that have undergone selection, the K_{S} and K_{A} description is limited to estimating the number of synonymous and non-synonymous nucleotide substitutions between exons of homologous genes.

Some approaches that exist are indirect measures of intrinsic adaptability at the genetic level. The PAM and BLOSUM matrices, for example, describe mutabilities between amino acids rather than between codons (Dayhoff *et al.*, 1978; Henikoff and Henikoff, 1992; Durbin *et al.*, 1998). Moreover, a matrix of pure mutational tendencies is ideally constructed from data gathered from non-selected genomic data, such as intron regions or pseudo-genes. Yang and Kumar have developed what is known as the Q matrix (Yang and Kumar, 1996). This matrix quantifies the underlying mutational pattern of nucleotide substitution. This 4×4 matrix, which deals with bases rather than codons, will be useful in our development. A codon mutation matrix based upon the assumption that the ratio of transition to transversion mutation rates is constant and that the ratio of nonsynonymous to synonymous mutation rates is constant has been developed (Goldman and Yang, 1994). This matrix can capture mutational data that are consistent with the assumption of equal transition to transversion and nonsynonymous to synonymous mutation rates. Our 64×64 matrix separates the species-specific mutation probabilities, and it additionally allows us to quantify the efficacy, type, and biases of subsequent codon mutation changes in the context of the genetic code.

In the context of pathogen and disease evolution, the mutation matrix can be a valuable

tool to quantify mutation probabilities and to enable the design of therapeutics and vaccines that would most effectively target disease epitopes that have the lowest chance of evolutionary escape (Freire, 2002). In the context of laboratory evolution of proteins, or protein molecular evolution (Patten *et al.*, 1997; Lutz and Benkovic, 2000; Petrounia and Arnold, 2000), knowing the tendencies of codons to mutate synonymously, conservatively, or non-conservatively would be helpful in experiment design.

2 Methods

2.1 The Codon Mutation Matrix

As an approximation, it is initially assumed that each base in a codon mutates independently. This allows the 64×64 codon mutation matrix to be constructed from the 4×4 base mutation matrix. In particular

$$T_{ij} = t_{i_1 j_1} t_{i_2 j_2} t_{i_3 j_3} \ , \tag{1}$$

where i is the number of the codon that will be mutated and j is the number of the codon that results after the mutation, with $1 \leq i, j \leq 64$. The codon is denoted by $i_1 i_2 i_3$, where i_1 is the first base in codon i, i_2 is the second base, and i_3 is the third base, with $1 \leq i_1, i_2, i_3 \leq 4$. Similarly, $j_1 j_2 j_3$ is the base triplet for codon j. The probability of a mutation from codon i to codon j in one round of replication is given by the codon mutation matrix T_{ij}. In this mathematical representation, the probability per round of no mutation is given by T_{ii}. Since either a mutation occurs or no mutation occurs, this matrix satisfies the constraint

$$\sum_{j=1}^{64} T_{ij} = 1 \quad \text{for all i} \ . \tag{2}$$

The probability per round of a mutation from one base to another is given by the base substitution matrix t. The base mutation matrix also satisfies conservation of probability $\sum_{j_1=1}^{4} t_{i_1 j_1} = 1$. This definition leads to what is known mathematically as a discrete-time Markov process. The base mutation matrix t can be constructed from information about the mutation frequency for the four bases, A, C, G, and T. The non-diagonal elements of t are derived from the 12 different independent rates of mutation. Typically the non-diagonal elements are small, since the rate of mutation is on the order of $10^{-2} - 10^{-6}$ per base per replication. The diagonal elements of the base mutation matrix are computed from the conservation of probability constraint. The 64×64 codon mutation matrix is then constructed from the 4×4 base mutation matrix by equation 1. Each element of the

64×64 matrix thus gives the probability per round of one codon mutating to another codon. One round, or codon mutation step, can include zero, one, two, or three simultaneous base mutations.

The assumption that DNA bases mutate independently can be refined in the presence of additional experimental data. It is known, for example, that flanking bases affect the base mutation rate in the hypervariable region of mouse antibodies (Smith *et al.*, 1996). Overall mutation rates have been measured for base triplets, and this information can be used to refine the codon mutation matrix. If ω_i is the observed mutation rate for codon i, the improved codon mutation matrix T' is defined as

$$T'_{ij} = \frac{\omega_i}{z} T_{ij} \ , \tag{3}$$

where z is a constant chosen so that the average mutation rate of the codons remains unchanged by this operation: $z = \sum_{i \neq j} w_i T_{ij} / \sum_{i \neq j} T_{ij}$. Alternatively, the assumption of equal transition to transversion and synonymous to nonsynonymous mutation rates may be used to generate a refined codon mutation matrix (Goldman and Yang, 1994), although this will not be done in the present work.

The codon mutation matrix differs from organism to organism and is constructed here for several specific systems. Since comparative trends are of interest, the overall average base mutation rate is set to be the same in all species, 2×10^{-5} per replication. A different average mutation rate for each species would simply adjust the overall scale of the codon mutation matrix. In each case, the base mutation matrix is first constructed from available data, and then equation 1 is used to construct the full codon mutation matrix.

The 64×64 codon mutation matrix contains a total of 4096 elements, each element calculated from Equation 1 or Equation 3. For each codon a synonymous, conservative, and non-conservative mutability is defined. The synonymous mutability, for example, is the sum of all of the elements of the codon mutation matrix that change a codon by a synonymous mutation. Similarly, the conservative mutability is the sum of all of the elements of the codon mutation matrix that change a codon by a conservative mutation. A conservative mutation occurs when a codon mutates to a codon that codes for a different amino acid that is, however, similar to the amino acid originally encoded. Amino acids are similar if they are in the same group, and there are seven groups: neutral and polar, positive and polar, negative and polar, nonpolar with ring, nonpolar without ring, cysteine, and stop. Substitutions that change the amino acid to a different group are defined as non-conservative, and substitutions that retain the encoded amino acid are defined as synonymous. Finally, the non-conservative mutability is the sum of all of the elements of the codon mutation matrix that change a codon by a non-conservative mutation. These three mutability values express the probability that a specific codon will mutate synonymously, conservatively, or non-conservatively in one round of

replication.

2.2 Systems Studied

The mutation frequencies of the *Taq* polymerase in error-prone PCR are available and can be extracted (Moore and Maranas, 2000). In the context of protein molecular evolution (Patten *et al.*, 1997; Lutz and Benkovic, 2000; Petrounia and Arnold, 2000), understanding the mutational process in error-prone PCR is especially important. The base mutation matrix for this, and the other systems, is available in the Supplementary Information. The three mutability values for each codon for this system are shown in Figure 1a.

The codon mutation matrix is also constructed for mutations in the intronic V regions of mouse antibodies (Smith *et al.*, 1996). Equation 3 is used to account for the effect of flanking bases in the mutation process, using JH/Jκ intronic data (Shapiro *et al.*, 1999). The mutability values for this system are shown in Figure 1b.

The data from non-long terminal repeat retrotransposable elements are used to construct the 4×4 base mutation matrix for *Drosophila* (Petrov and Hartl, 1999). Only the data from the terminal branches, representing "dead-on-arrival," nonfunctional copies that are unconstrained by selection were used. These copies evolve as pseudo-genes.

The last system for which a codon mutation matrix is constructed is mitochondrial DNA from *Haemonchus contortus* (Blouin *et al.*, 1998). This is a nematode in the same subclass Rhabditia as *Caenorhabditis elegans*. Coding regions of mtDNA were used to allow for comparison with codon usage data available in the literature. The base mutation matrix obtained from this data is treated as applicable to nuclear DNA, and so the standard genetic code is used. While use of intronic data from *C. elegans* would be preferable, such data are difficult to collect due to the extensive divergence between *C. elegans* and its near relative, *C. briggsae* (T. Blumenthal, personal communication, 2001). The mutation rate data estimated by the mtDNA mutation rates will not play an essential role in the analysis.

2.3 The No-Bias Codon Mutabilities

We are looking for biases in the underlying mutation rates of the replication machinery, not for biases in the genetic code itself. The genetic code biases–that hydrophobic residues tend to mutate to hydrophobic residues and that hydrophilic residues tend to mutate to hydrophilic residues–are well known (Woese, 1965; Epstein, 1966; Goldberg and Wittes, 1966; Fitch, 1966; Volkenstein, 1994). To investigate biases other than those induced by the genetic code, a refine-

ment to the codon mutability plots is made. This refinement subtracts from each mutability a value termed as the "no-bias" value. The "no-bias" value comes from a 64×64 matrix that is created by using a 4×4 matrix where each non-diagonal term has equal mutation frequencies, *e.g.* equal transition and transversion rates. In other words, the no-bias plots indicate which empirically derived mutabilities are above or below those expected if all base substitutions were equally likely. This matrix serves as a baseline for unbiased mutation rates within the context of the genetic code. This no-bias transformation is not a correction: it is a refined way to do the analysis. The overall mutation rate of the no-bias codon mutation matrix is made to be same as that of the original codon mutation matrix. Synonymous, conservative, and non-conservative mutabilities are calculated from this baseline 64×64 matrix and subtracted from the original mutabilities, Figure 2.

3 Results

3.1 Modulation of Codon Mutation Rates

Error-prone PCR, while not a pure biological system, is a central tool and serves as an excellent example of the power of our approach. Figure 2a immediately reveals that for error-prone PCR, the codons that code for polar amino acids have low relative conservative and non-conservative mutabilities. That is, these mutabilities are much lower than what would be expected under unbiased conditions. For the codons that code for the nonpolar amino acids, on the other hand, a different pattern is observed. In this case, the conservative and non-conservative mutabilities are higher than the baseline values generated from equal mutation rates. Note that because of the factorization in Equation 1, our theory describes the biasing effect of base mutations, and the "reading frame" of *Taq* does not matter. In Figures 1a and 2a we are showing the effect of these biased base mutations when the ribosome reads the exons in frame.

To study the possible effects of mutability modulation in a natural population undergoing rapid, active evolution, the mouse V regions are examined with the 64×64 mutation matrix approach. Interestingly, higher conservative and non-conservative mutabilities are observed for the polar amino acids compared to the nonpolar amino acids, Figure 2b. We quantify the statistical significance of these results by computing the probability per round that a random base mutation matrix would lead to a ratio of mutation rates between the polar groups and the nonpolar groups that is as great or greater than that observed. That is, we take the ratio of the sum of the conservative and non-conservative mutabilities from Figure 1 for these two groups. The probability by chance that this ratio is as large or larger than that in Figure 1b is 8.6%. From this extremely conservative statis-

tic, it can be concluded that the pattern of increased mutability of polar amino acids is statistically significant to the level of 91%. We also perform this same calculation using another, independent estimate of the base mutation matrix for mouse V regions (Neuberger and Milstein, 1995). The probability by chance that the ratio of conservative and non-conservative mutabilities for a random matrix is larger than that given by this new matrix is 5.3%. This result is, thus, significant to the level of 95%. It is interesting to note that if one assumed the experimentally measured base mutation matrices were random, *i.e.* dominated by experimental noise, the probability that two random such matrices would give a ratio as large or larger than that observed in Figure 1b is $0.086^2 = 0.7\%$.

It is difficult to measure experimentally exact mutation rates. Thus, the sensitivity of the codon mutation matrix to changes in the base substitution rates is of interest. In order to test the robustness of our findings for *Taq* to experimental noise, a random number is added or subtracted from each of the twelve off-diagonal, independent values in the 4×4 base mutation matrix. This random number is generated from a Gaussian distribution with zero mean and a standard deviation that is equal to a given percentage of the average mutation rate. This procedure generates a new 4×4 base mutation matrix, from which a new 64×64 codon mutation matrix is calculated. To determine if the mutability bias patterns found in Figure 2a is perturbed by the addition of noise, codon mutability plots are created with the new codon mutation matrix. This plot displays the pattern observed in Figure 2a until the noise overwhelms the signal. The pattern from Figure 2a is still evident up to noise levels of 50% of the average mutation rate, disappearing only when the noise reaches 60% (Tan, 2002). An analagous calculation was performed for the mouse V region system, and again the pattern in Figure 2b persisted up to noise levels of 50% of the average mutation rate, disappearing only when the noise reaches 60% (Tan, 2002). Thus, the observed trends in Figure 2 are rather robust to the presence of experimental noise.

One might wonder whether this pattern of increased non-synonymous mutabilities of charged residues would survive in other mouse or mammalian genes. Figure 3 shows the no-bias codon mutability plot derived from non-immune-system gene mutation rates from human B cells. Data are from (Shen *et al.*, 2000). As expected, there is no overall pattern. A quantitative comparison to the polar to nonpolar ratio of conservative and non-conservative mutabilities calculated for Figure 1b shows that in this case the probability that a random base mutation matrix has a value higher than that observed in Figure 3 is 25%. Thus, the increase in the non-synonymous mutability of the mammalian, immunoglubulin V region in Figure 1b is unique and statistically significant.

Further analysis of the codon mutation matrices was done by combining mutability information with codon usage information. Codon usage is necessary to determine via the mutation matrix the average rate of mutation of a gene, since the total rate of mutation depends on both the muta-

tion rate per codon and on which codons are present. By summing the product of the RSCU value (Sharp *et al.*, 1986) and the synonymous mutability for all the codons that code for a given amino acid, the synonymous mutability of amino acid α is calculated:

$$\text{synonymous mutability}(\alpha) = \sum_{i \in \alpha} p_i^\alpha \times \text{synonymous mutability}(i) \ , \tag{4}$$

where the synonymous mutability of codon i is taken from Figures 1a–1c, and the codon usage p_i^α is taken from the experimental RSCU values (Duret and Mouchiroud, 1999). The synonymous mutability of amino acids is observed to be higher in the short genes than in the long genes for the nematode, Figure 4. Indeed, of the amino acids, only arginine has a demonstrably lower synonymous mutability for the short genes, as seen in Figure 4. We calculate the probability that the observed increase in synonymous mutability is due to chance. The probability of 17 or more amino acids showing this trend out of 18 by chance is $[\binom{18}{18} + \binom{18}{17}]2^{-18} = 7.2 \times 10^{-5}$. Making the same plot for the nematode, one observes the pattern to be even more striking (Tan, 2002; Blouin *et al.*, 1998) (data not shown). Indeed, of the amino acids, only proline has a demonstrably lower synonymous mutability for the short genes, and only two other amino acids have roughly the same synonymous mutability in short and long genes. The probability of 15 or more amino acids showing this trend out of 16 by chance is $[\binom{16}{16} + \binom{16}{15}]2^{-16} = 2.6 \times 10^{-4}$.

While there are selective pressures on synonymous codon usage, such as preference for tRNAs at different levels of abundance, it seems unlikely that there would be a selection on the quantity synonymous mutation rate, in and of itself, that is significant enough to cause the observed correlation. In other words, there are known to be selective pressures on codon usage. What is not clear is why there should be selective pressure on synonymous mutation rate itself. There is selection pressure on the ability to adapt, however. In order for short genes to evolve at an overall rate comparable to that of long genes, the mutation rate per base would have to be higher in short genes. If one assumes that on average there is a certain number of mutations needed to effect functional adaptation of a protein, and that short proteins and long proteins need to evolve at roughly similar rates, this then implies that short proteins need a higher per base rate of evolution than long proteins—because they are shorter, and the evolution rate of a gene is the evolution rate per base times the number of bases. Thus, the evolution rate per base must be higher for shorter proteins. In contrast to Figure 4, however, a correlation between conservative or non-conservative mutation rate and gene length was not observed for either *Drosophila* or the nematode (data not shown).

3.2 Modulation of Recombination Rates

An alternative means of evolution is recombination, and recombination rates are known to be correlated with codon usage bias (Comeron *et al.*, 1999). Selection pressure on short genes for greater evolvability could favor a higher recombination rate per base, thus allowing short genes to evolve at a rate comparable to that of long genes. It would be unfavorable if evolution for higher recombination rates led to lower conservative or non-conservative mutation rates. C+G content is known to be a rough measure of recombination rate (Eyre-Walker, 1993; Comeron and Kreitman, 2000; Duret *et al.*, 2000; Birdsell, 2002). In other words, the correlation between C+G content and recombination rate is strong enough that C+G content is now felt to be a useful maker of local recombination rate (Fullerton *et al.*, 2001; Birdsell, 2002). Interestingly, we find that C+G is positively correlated with all three mutation rates and is most highly correlated with synonymous mutation rate. Moreover, as Figure 5a shows, the codon usage of short genes is such that a higher per base rate of estimated recombination is favored. The recombination rate of amino acid α is estimated by

$$\text{estimated recombination rate}(\alpha) = \sum_{i \in \alpha} p_i^{\alpha} \times (\text{number of C or G bases in codon } i) \, , \qquad (5)$$

where the codon usage p_i^{α} is taken from the experimental RSCU values (Duret and Mouchiroud, 1999). In Figure 5a, only one exception, for proline, is found to the general pattern. As Figure 5b shows, a similar correlation between codon usage and enhanced estimated recombination frequency is also observed in *Drosophila*. No exceptions to the general pattern are found in Figure 5b. Finally, Figure 5c shows the estimated recombination rate for *A. thaliana*. In Figure 5c, only one exception, for glycine, is found to the general pattern. Considering all three species, the probability of 52 or more amino acids showing this trend out of 54 by chance is $[\binom{54}{52} + \binom{54}{53} + \binom{54}{54}]2^{-54} = 8.2 \times 10^{-14}$. The pattern is, thus, highly statistically significant. One explanation for the observed codon usage of short, high-expression genes is selective pressure on crossover frequency. On a long time scale, other factors such as neutral evolution and rearrangements become important, and this is likely the reason for the relatively modest shifts in the codon usage observed in Figure 5.

In Figure 6a is shown the *measured* recombination rate versus protein length for genes in *Drosophila* at high expression levels (Hey and Kliman, 2002) (EST > 50). In this species, codon bias is observable for genes at all recombination levels. The correlation between codon bias and recombination rate is seen, however, only when the latter is low rates (Hey and Kliman, 2002; Marais and Piganeau, 2002). Figure 6 is, therefore, made only for recombination rates less than 1 centimorgan per megabase. A negative correlation between recombination rate and protein length is observed. In Figure 6c, the *measured* recombination rate versus protein length is shown for *C.*

elegans for genes at high expression levels (Marais and Piganeau, 2002). A clear negative correlation between recombination rate and gene length is again observed.

4 Discussion

4.1 Selective Pressures on Codon Mutation Rates

It was found that for the Taq polymerase, nonpolar amino acids are mutated at an elevated rate. Nonpolar amino acids are more frequently present in the interior cores of proteins, and mutations of these amino acids more often lead to dramatic rearrangements of the protein structure. The pattern in the error-prone PCR mutation plot suggests that the mutations that occur will tend to cause larger changes in the structure of the encoded protein. It is becoming more accepted that large mutation events such as transpositions, horizontal transfers, gene exchange, and non-conservative mutations are necessary for dramatic evolution. This was shown quantitatively in (Bogarad and Deem, 1999). Non-conservative mutations in the core of the protein would be one of the most dramatic amino acid substitution moves possible and can be considered to search the protein sequence space most broadly. In other words, under error-prone conditions, the *Taq* polymerase favors codons for the nonpolar amino acids that mutate non-conservatively. This property of error-prone PCR greatly enhances the ability of this method to improve protein function effectively by forcing the search of greater regions of tertiary fold space. Moreover, the average mutational tendencies of *Taq* can be modulated by codon usage. Table 1 defines codons by their tendencies to evolve under error prone conditions. These data can be useful in the design of protein evolution experiments, especially when trying to evolve new motifs *ab initio*.

It was found that for V regions of mouse antibodies there is an increase in the mutation rate of the charge amino acids. These trends are not sensitive to whether equation 1 or equation 3 is used to model the mutation matrix or whether the mutation data are taken from (Smith *et al.*, 1996; Shapiro *et al.*, 1999) or from (Neuberger and Milstein, 1995). Antibody V regions undergo DNA swapping of gene fragments in order to create the primary repertoire needed to develop resistance to disease. Therefore, base mutations that alter the framework of the proteins become less necessary. More significant are mutations that lead to a greater binding affinity. In protein-protein complexes, a positive correlation is observed between binding affinity and the number of ionic interactions spanning an interface (Sheinerman *et al.*, 2000; Xu *et al.*, 1997). Thus for the polar amino acids participating in binding, high conservative and non-conservative mutabilities would be most favorable, since such characteristics would enable more efficient searching of sequence space to optimize binding.

4.2 Selective Pressures on Recombination Rates

Previously, a correlation between codon usage bias and gene length had been observed in the species considered here (Duret and Mouchiroud, 1999). Several mechanisms that might explain the increased codon bias in short genes were considered, including biased tRNA levels, but all predicted increased bias for longer genes, in contrast to the greater observed bias for shorter genes (Duret and Mouchiroud, 1999). We suggest that codon usage in short genes in these species has evolved due to selection for increased recombination frequency, Figure 6. This mechanism is consistent with previously observed positive correlations between recombination rate and codon usage bias and with previously observed negative correlations between gene length and codon usage bias (Comeron *et al.*, 1999; Comeron and Kreitman, 2000). The observed correlation between codon usage and synonymous mutation rate, Figure 4, may be a byproduct of selection on recombination rate, as synonymous mutation rate is positively correlated with C+G content ($R = 0.62$ for *Drosophila*, and $R = 0.51$ for the nematode).

In (Duret and Mouchiroud, 1999), the codon usage bias was highest for those genes at high expression levels, and Figure 5 is based upon those data. In fact, the expression level was estimated in (Duret and Mouchiroud, 1999) from the frequency with which those genes were observed in the EST database. It is possible that certain genes may be overrepresented in the EST database, in a way that is correlated with the gene length. If this unknown bias were the cause of the correlation in Figure 5, then the opposite or no correlation would be expected to be observed for genes at low expression. In fact (data not shown), the same patterns observed in Figure 5a are observed when codon usage for the genes at low (bottom 1/3 of genes with non-zero EST abundance) rather than high (top 1/3 of genes with non-zero EST abundance) expression levels are used: Among the 54 amino acids, only three have lower estimated recombination rates for the short genes at low expression levels than for the long genes at low expression levels.

It might be argued that to be fully consistent with our theory, the relevant recombination rate is that of the whole gene, divided by the coding length of the gene. This quantity is slightly different from the quantity plotted in Figure 6ac because the intron to exon composition of genes could vary systematically with length. This concern has been addressed in Figure 6b, where recombination rate times gene length divided by coding length has been plotted. The same negative correlation between recombination rate and gene length is again observed.

For our explanation to be consistent, it must be the case that *Drosophila* and *C. elegans* are, in some sense, mutationally starved. The very existence of the Hill-Robertson effect in these species (Marais and Piganeau, 2002) implies that this is the case, because it implies that point mutation is insufficient to evolve linked genes, and that recombination is necessary to break the linkage.

The existence of related effects, such as interference selection (Comeron and Kreitman, 2002), provides additional evidence for the same reasons. Finally, the fact that codon bias is observable only for genes at low recombination rates in *Drosophila*, less than 1 (Marais and Piganeau, 2002) or 1.5 (Hey and Kliman, 2002) cM/Mb, provides additional indirect evidence that the selective pressure to increase evolution rates is strongest where evolution is the slowest.

5 Conclusion

Previous treatments of the evolutionary biology of codon usage have largely ignored the possibility that codon usage could *affect* mutation or recombination rates and have primarily focused on using codon usage as a measure of selection. We here suggest that not only can codon usage affect mutation and recombination rates but also codon usage has been selected to enhance functional gene adaptation within the context of the genetic code. This line of reasoning is in accord with strategies for optimized design of experimental protein molecular evolution protocols, where speed of evolution is an explicit goal (Bogarad and Deem, 1999; Moore and Maranas, 2002).

In Nature there are numerous examples of exploiting codon potentials in ongoing evolutionary processes. In the V regions of encoded antibodies, high-potential serine codons such as AGC are found predominately in the encoded CDR loops while the encoded frameworks contain low-potential serine codons such as TCT (Wagner *et al.*, 1995). Unfortunately, antibodies and drugs are often no match for the hydrophilic, high-potential codons of "error-prone" pathogens. The dramatic mutability of the HIV gp120 coat protein is one such example. One can envision a scheme for using codon potentials to target disease epitopes that mutate rarely (*i.e.*, low-potential) and unproductively (*i.e.*, become stop, low-potential, or structure-breaking codons). Such a therapeutic scheme should be generally useful against diseases that use error prone replication to escape therapeutic treatments or vaccines.

6 Acknowledgment

This research was supported by the National Institutes of Health and the National Science Foundation.

References

Altenberg L (1994) The evolution of evolvability in genetic programming. In: Kinnear KE (ed.), *Advances in Genetic Programming*. MIT Press, Cambridge, MA, pp. 47–74

Birdsell JA (2002) Integrating genomics, bioinformatics, and classical genetics to study to effects of recombination on genome evolution. Mol Biol Evol 19:1181–1197

Blouin MS, Yowell CA, Courtney CH, Dame JB (1998) Substitution bias, rapid saturation, and the use of mtDNA for nematode systematics. Mol Biol Evol 15:1719–1727

Bogarad LD, Deem MW (1999) A hierarchical approach to protein molecular evolution. Proc Natl Acad Sci USA 96:2591–2595

Bull HJ, Lombardo MJ, Rosenberg SM (2001) Stationary-phase mutation in the bacterial chromosome: Recombination protein and DNA polymerase IV dependence. Proc Natl Acad Sci USA 98:8334–8341

Comeron JM, Kreitman M (2000) The correlation between intron length and recombination in *Drosophila*: Dynamic equilibrium between mutational and selective forces. Genetics 156:1175–1190

Comeron JM, Kreitman M (2002) Population, evolutionary and genomic consequences of interference selection. Genetics 161:389–410

Comeron JM, Kreitman M, Aguade M (1999) Natural selection on synonymous sites is correlated with gene length and recombination in *Drosophila*. Genetics 151:239–249

Dayhoff MO, Schwartz RM, Orcutt BC (1978) A model of evolutionary change in proteins. In: *Atlas of Protein Sequence and Structure*, National Biomedical Research Foundation, vol. 5, pp. 345–352

Durbin R, Eddy S, Krogh A, Mitchison G (1998) Biological Sequence Analysis. Cambridge University Press, Cambridge, United Kingdom

Duret L, Marais G, Biémont C (2000) Transposons but not retrotransposons are located preferentially in regions of high recombination rate in *C. elegans*. Genetics 156:1661–1669

Duret L, Mouchiroud D (1999) Expression pattern and, surprisingly, gene length shape codon usage in *Caenorhabditis*, *Drosophila*, and *Arabidopsis*. Proc Natl Acad Sci USA 96:4482–4487

Epstein CJ (1966) Role of the amino acid ‘code’ and of selection for conformmation in the evolution of proteins. Nature 210:25–28

Eyre-Walker A (1993) Recombination and mammalian genome evolution. Proc R Soc Lond Ser B Biol Sci 252:237–243

Fitch WM (1966) The relation between frequencies of amino acids and ordered trinucleotides. J Mol Biol 16:1–16

Freire E (2002) Designing drugs against heterogeneous targets. Nat Biotech 20:15–16

Friedberg EC, Feaver WJ, Gerlach VL (2000) The many faces of DNA polymeraces: Strategies for mutagenesis and for mutational avoidance. Proc Natl Acad Sci USA 97:5681–5683

Fullerton SM, Carvalho AB, Clark AG (2001) Local rates of recombination are positively correlated with GC content in the human genome. Mol Biol Evol 18:1139–1142

Goldberg AL, Wittes R (1966) Genetic code: Aspects of organization. Science 153:420–422

Goldman N, Yang Z (1994) A codon-based model of nucleotide substitution for protein-coding DNA sequences. Mol Biol Evol 17:32–43

Henikoff JG, Henikoff S (1992) Amino acid substitution matrices from protein blocks. Proc Natl Acad Sci USA 89:10915–10919

Hey J, Kliman RM (2002) Interactions between natural selection, recombination, and gene density in the genes of Drosophila. Genetics 160:595–608

Kepler TB (1997) Codon bias and plasticity in immunoglobulins. Mol Biol Evol 14:637–643

Lathrop RH, Pazzani MJ (1999) Combinatorial optimization in rapidly mutating drug-resistant viruses. J Comb Optim 3:301–320

Lawrence JG (1997) Selfish operons and speciation by gene transfer. Trends Microbiol 5:355–359

Li W, Wu C, Luo C (1985) A new method for estimating synonymous and nonsynonymous rates of nucleotide substitution considering the relative likelihood of nucleotide and codon changes. Mol Biol Evol 2:150–174

Lutz S, Benkovic SJ (2000) Homology-independent protein engineering. Curr Opin Biotech 11:319–324

Marais G, Piganeau G (2002) Hill-Robertson interference is a minor determinant of variations in codon bias across *Drosophilia Melanogaster* and *Caenorhabditis elegans* genomes. Mol Biol Evol 19:1399–1406

Moore GL, Maranas CD (2000) Modeling DNA mutation and recombination for directed evolution experiments. J Theor Biol 205:483–503

Moore GL, Maranas CD (2002) eCodonOpt: A systematic computational framework for optimizing codon usage in directed evolution experiments. Nucleic Acids Res 30:2407–2416

Neuberger MS, Milstein C (1995) Somatic hypermutation. Curr Opin Immunol 7:248–254

Ofria C, Adami C, Collier TC, Hsu GK (1999) Evolution of differentiated expression patterns in digital organisms. Adv Artific Life 1674:129–138

Patel PH, Kawate H, Adman E, Ashbach M, Loeb LA (2001) A single highly mutable catalytic site amino acid is critical for DNA polymerase fidelity. J Biol Chem 276:5044–5051

Patten PA, Howard RJ, Stemmer WPC (1997) Applications of DNA shuffling to pharmaceuticals and vaccines. Curr Opin Biotech 8:724–733

Pennisi E (1998) Molecular evolution–How the genome readies itself for evolution. Science 281:1131–1134

Peper JW (2003) The evolution of evolvability in genetic linkage patterns. Biosystems 69:115–126

Petrounia IP, Arnold FH (2000) Designed evolution of enzymatic properties. Curr Opin Biotech 11:325–330

Petrov DA, Hartl DL (1999) Patterns of nucleotide substitution in *Drosophila* and mammalian genomes. Proc Natl Acad Sci USA 96:1475–1479

Plotkin JB, Doshoff J (2003) Codon bias and frequency-dependent selection on the hemagglutinin epitopes of influenza A virus. Proc Natl Acad Sci USA 100:7152–7157

Shapiro GS, Aviszus K, Ikle D, Wysocki LJ (1999) Predicting regional mutability in antibody V genes based solely on di- and trinucleotide sequence composition. J Immunol 163:259–268

Sharp PM, Tuohy TMF, Mosurski KR (1986) Codon usage in yeast: Cluster analysis clearly differentiates highly and lowly expressed genes. Nucleic Acids Res 14:5125–5143

Sheinerman FB, Norel R, Honig B (2000) Electrostatic aspects of protein-protein interactions. Curr Opin Struct Biol 10:153–159

Shen HM, Michael N, Kim N, Storb U (2000) The TATA binding protein, c-Myc and survivin genes are not somatically hypermutated, while Ig and BCL6 genes are hypermutated in human memory B cells. Int Immun 12:1085–1093

Smith DS, Creadon G, Jena PK, Portanova JP, Kotzin BL, Wysocki LJ (1996) Di- and trinucleotide target preference of somatic mutagenesis in normal and autoreactive B cells. J Immunol 156:2642–2652

Storb U (2001) DNA polymerases in immunity: Profiting from errors. Nat Immunol 2:484–485

Sutton MD, Walker GC (2001) Managing DNA polymerases: Coordinating DNA replication, DNA repair, and DNA recombination. Proc Natl Acad Sci USA 98:8342–8349

Tan T (2002) Ph.D. Dissertation. The Codon Mutation Matrix in the Context of Protein Molecular Evolution. UCLA

Thearling K, Ray TS (1997) Evolving parallel computation. Complex Systems 10:229–237

Travis JMJ, Travis ER (2002) Mutator dynamics in fluctuating environments. Proc Roy Soc B London 269:591–597

Volkenstein MV (1994) Physical Approaches to Biological Evolution. Springer-Verlag, New York

Wagner GP, Altenberg L (1996) Perspective: Complex adaptations and the evolution of evolvability. Evolution 50:967–976

Wagner SD, Milstein C, Neuberger MS (1995) Codon bias targets mutation. Nature 376:732

Woese CR (1965) On the evolution of the genetic code. Proc Natl Acad Sci USA 54:1546–1552

Xu D, Lin SL, Nussinov R (1997) Protein binding versus protein folding: The role of hydrophobic bridges in protein association. J Mol Biol 265:68–84

Yang Z, Kumar S (1996) Approximate methods for estimating the pattern of nucleotide substitution and the variation of substitution rates among sites. Mol Biol Evol 13:650–659

Table 1: Table of codon classifications for the error-prone PCR system.

	synonymous	conservative	non-conservative
Cys			TGC, TCT
Ser	TCA, TCT	TCC, TCG	AGC, AGT
Thr	ACA	ACC, ACG, ACT	
Pro	CCA, CCC, CCT	CCG	
Ala	GCA, GCT	GCC, GCG	
Gly	GGA, GGT		GGC, GGG
Asn			AAC, AAT
Gln			CAA, CAG
Asp			GAC, GAT
Glu			GAA, GAG
His			CAC, CAT
Arg	CGA, CGT		AGA, AGG, CGC
			CGG
Lys			AAA, AAG
Met		ATG	
Ile		ATA	ATC, ATT
Leu	CTA		CTC, CTG, CTT
			TTA, TTG
Val			GTA, GTC, GTG
			GTT
Phe			TTC, TTT
Tyr			TAC, TAT
Trp			TGG
Stop			TAA, TAG, TGA

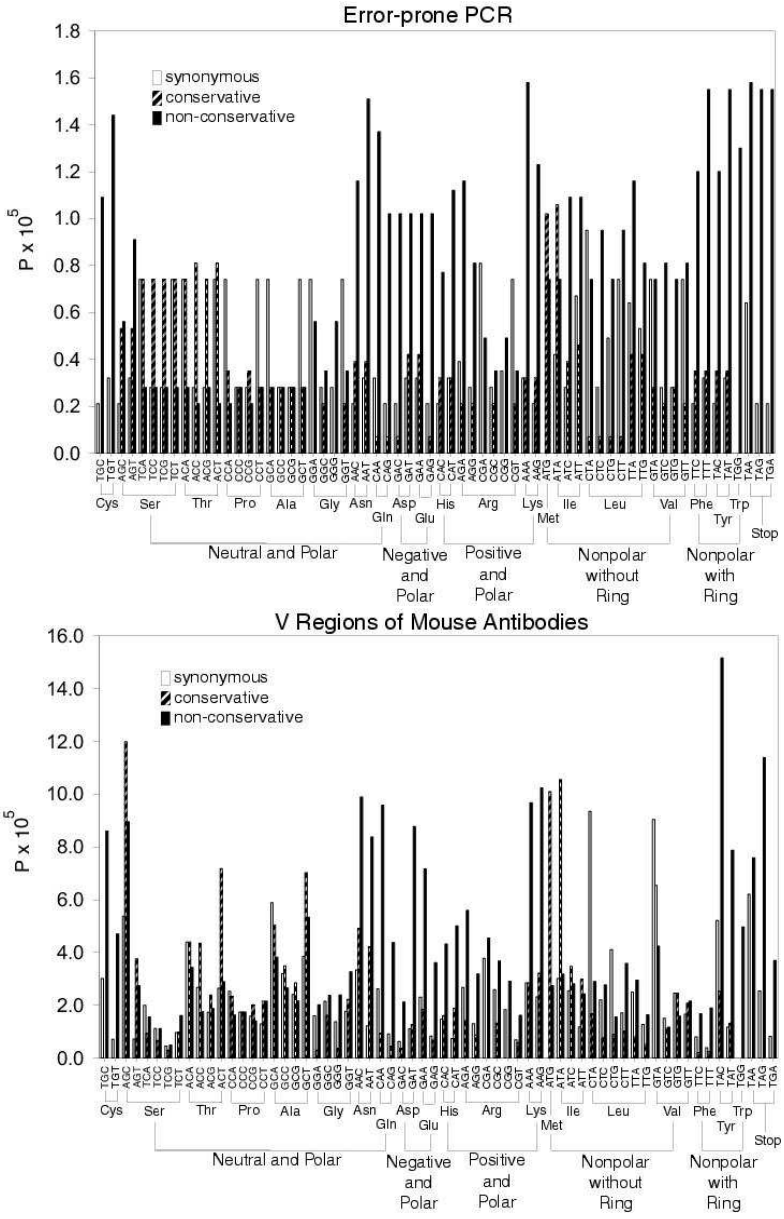

Figure 1: The codon mutability plot for a) error-prone PCR and b) V regions of mouse antibodies. Each plot displays the synonymous, conservative, and non-conservative mutabilities for each codon.

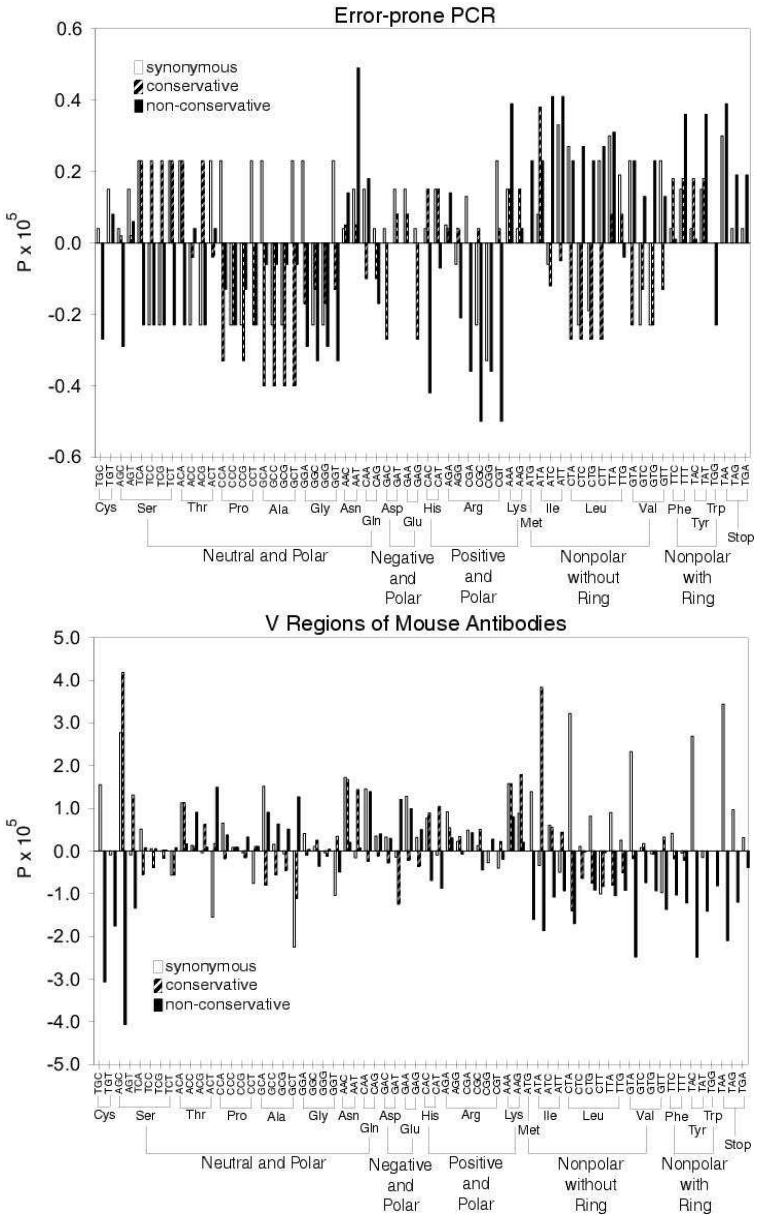

Figure 2: The no-bias plot for a) error-prone PCR and b) V regions of mouse antibodies. This refinement to the codon mutability plots takes into account the baseline substitution rate due to the inherent structure in the genetic code.

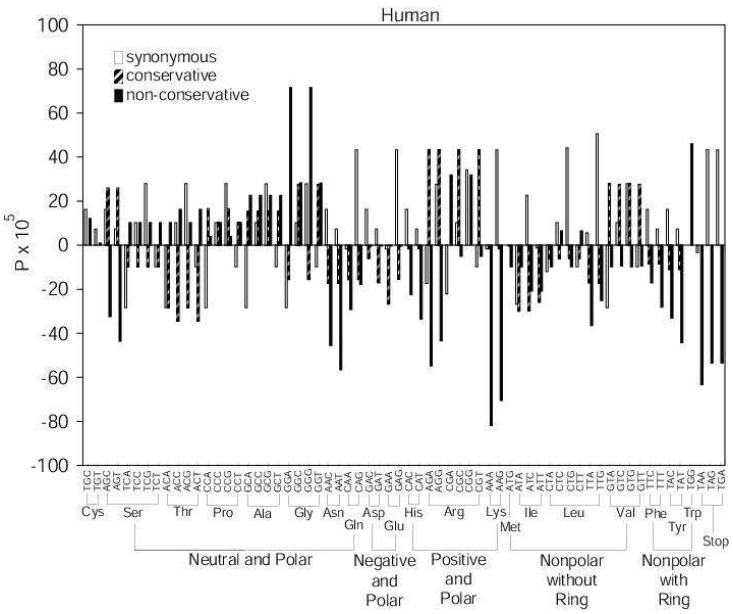

Figure 3: No-bias plot for the non-immune-system genes c-Myc, survivin1, survivin2, and TBP in human B cells.

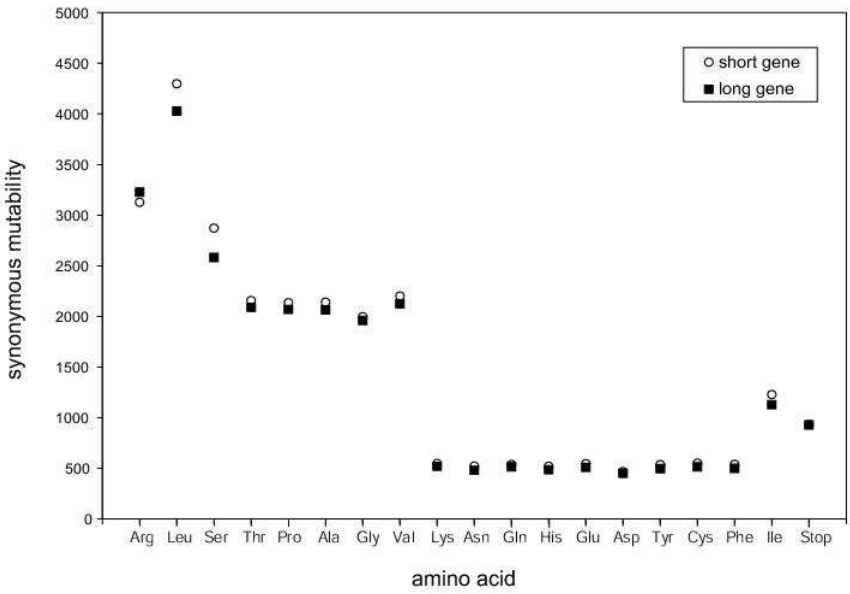

Figure 4: Synonymous mutabilities for *Drosophila* for amino acids in short (< 333 amino acids) and long (> 570 amino acids) genes at high expression levels (top 1/3 of genes with non-zero EST abundance). Higher values of synonymous mutability are observed in the shorter genes.

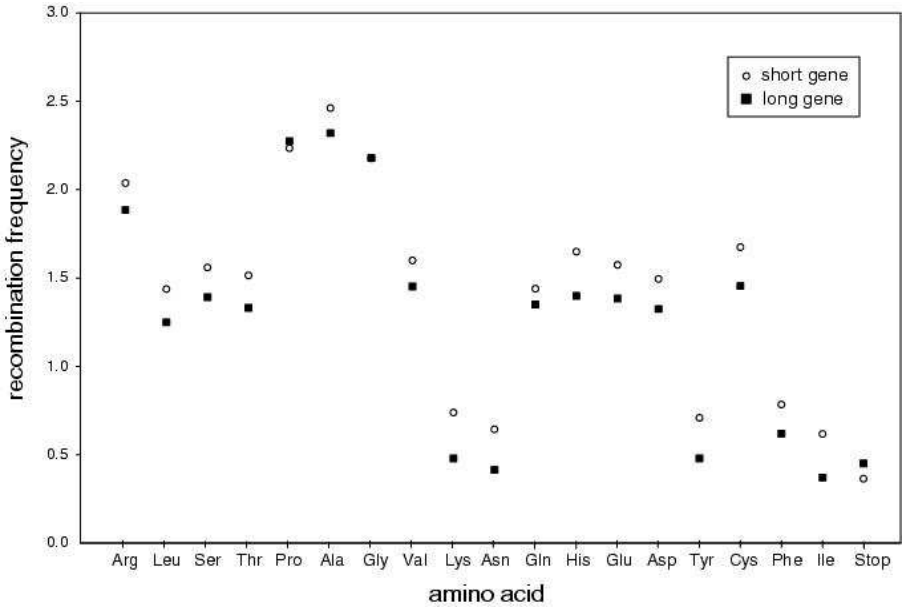
short gene
long gene
recombination frequency
3.0
2.5
2.0
1.5
1.0
0.5
0.0
Arg Leu Ser Thr Pro Ala Gly Val Lys Asn Gln His Glu Asp Tyr Cys Phe Ile Stop
amino acid

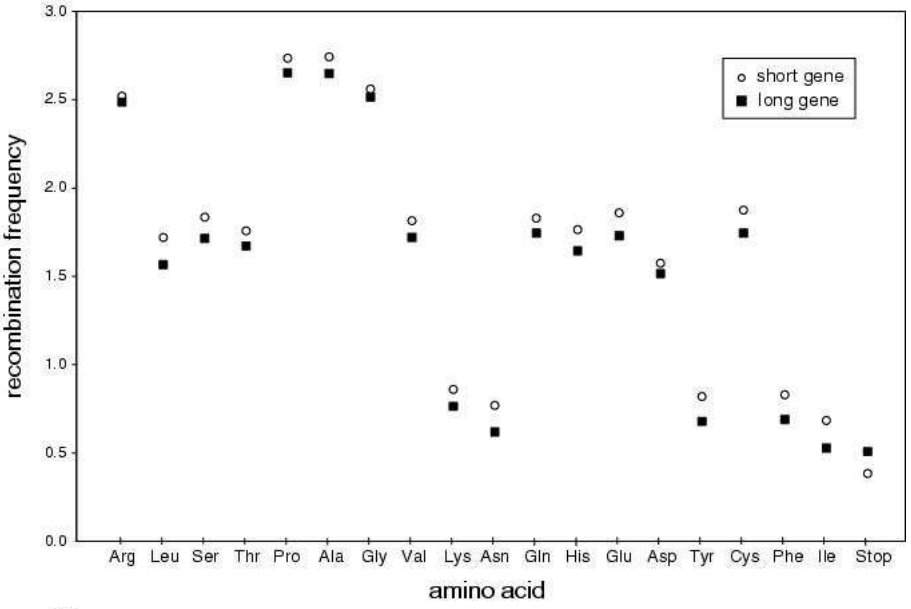
short gene
long gene
recombination frequency
3.0
2.5
2.0
1.5
1.0
0.5
0.0
Arg Leu Ser Thr Pro Ala Gly Val Lys Asn Gln His Glu Asp Tyr Cys Phe Ile Stop
amino acid

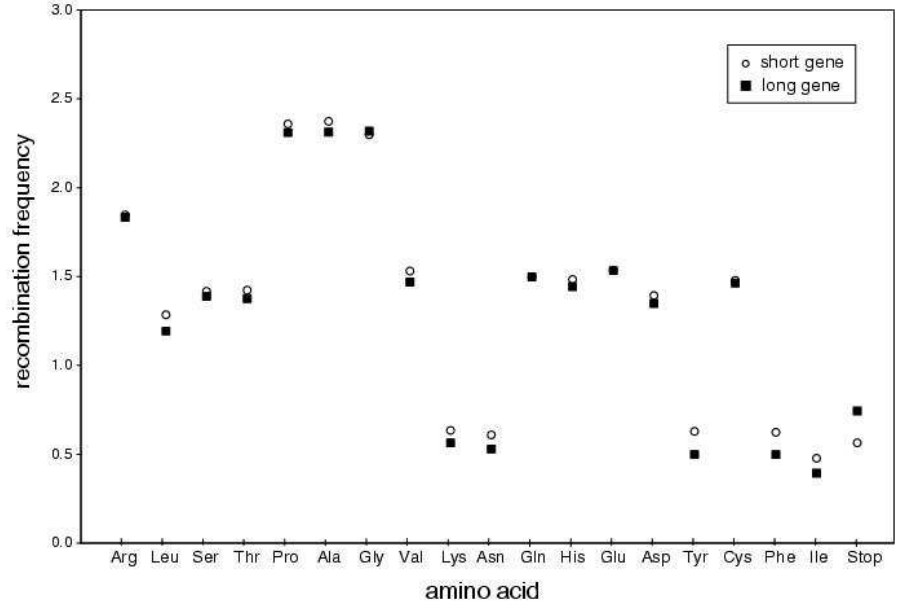
short gene
long gene
recombination frequency
3.0
2.5
2.0
1.5
1.0
0.5
0.0
Arg Leu Ser Thr Pro Ala Gly Val Lys Asn Gln His Glu Asp Tyr Cys Phe Ile Stop
amino acid

Figure 5: Estimated recombination frequency for a) *C. elegans*, b) *D. melanogaster*, and c) *A. thaliana* for amino acids in short (< 333 amino acids) and long (> 570 amino acids) genes at high expression levels (top 1/3 of genes with non-zero EST abundance). Higher values of estimated recombination frequency are observed in the shorter genes. Recombination frequency is estimated by the sum over all codons encoding a given amino acid of the observed codon usage times the number of C and G bases in the codon.

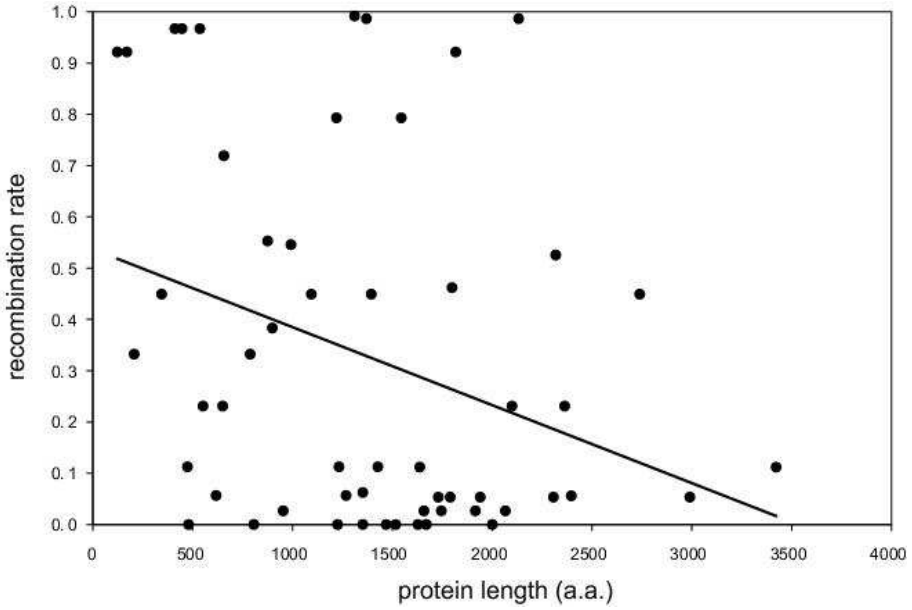
recombination rate
1.0
0.9
0.8
0.7
0.6
0.5
0.4
0.3
0.2
0.1
0.0
0
500
1000
1500
2000
2500
3000
3500
4000
protein length (a.a.)

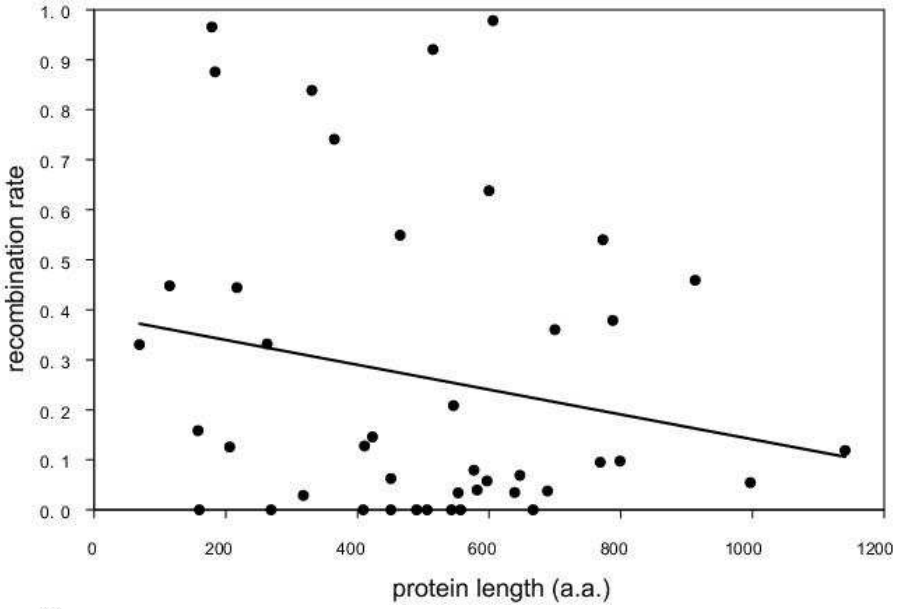
recombination rate
1.0
0.9
0.8
0.7
0.6
0.5
0.4
0.3
0.2
0.1
0.0
0
200
400
600
800
1000
1200
protein length (a.a.)

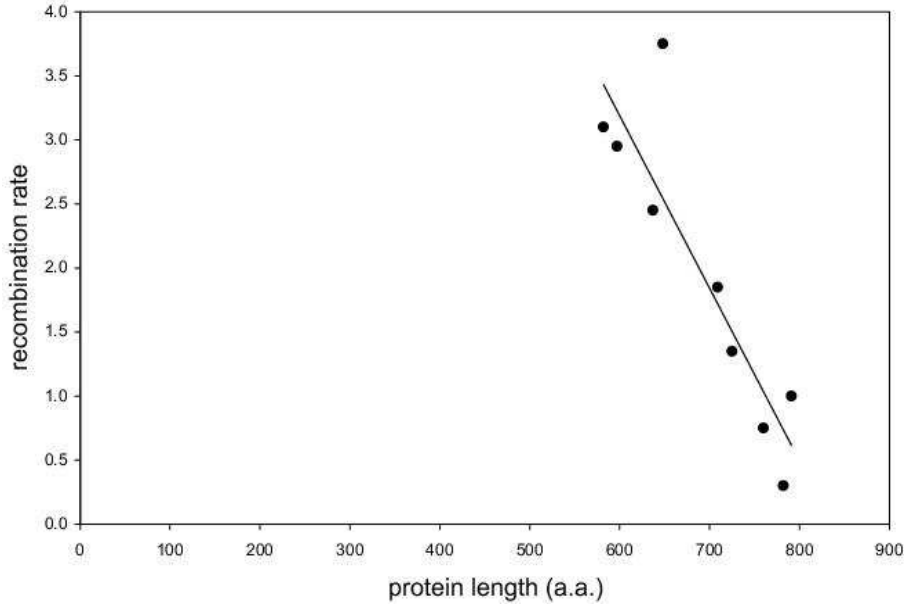
recombination rate
4.0
3.5
3.0
2.5
2.0
1.5
1.0
0.5
0.0
0
100
200
300
400
500
600
700
800
900
protein length (a.a.)

Figure 6: Measured recombination frequency (centimorgan/megabase) as a function of protein length (amino acids) for a) *D. melanogaster*, b) *D. melanogaster*, where recombination frequency is modifed to account for intron to exon base composition, $R\times(\mathrm{gene\ length})/(\mathrm{coding\ length})$, and c) *C. elegans*. Also shown are linear fits to the data; the correlation coefficients are a) $R = -0.32$, b) $R = -0.20$, and c) $R = -0.89$. All data are for genes at high expression levels. Data in a) and b) are taken from (Hey and Kliman, 2002). Data in c) are replotted from the binned data of (Marais and Piganeau, 2002).

Supplementary Information

Table 2: The base mutation matrix t for error-prone PCR (Moore and Maranas, 2000).

	A	C	G	T
A	1–7.4×10^{-6}	7.0×10^{-7}	3.2×10^{-6}	3.5×10^{-6}
C	7.0×10^{-7}	1–2.8×10^{-6}	0	2.1×10^{-6}
G	2.1×10^{-6}	0	1–2.8×10^{-6}	7.0×10^{-7}
T	3.5×10^{-6}	3.2×10^{-6}	7.0×10^{-7}	1–7.4×10^{-6}

Table 3: The base mutation matrix t for V regions of mouse antibodies (Smith *et al.*, 1996; Shapiro *et al.*, 1999).[a]

	A	C	G	T
A	1–3.327×10^{-5}	6.550×10^{-6}	1.847×10^{-5}	8.250×10^{-6}
C	4.580×10^{-6}	1–2.597×10^{-5}	4.370×10^{-6}	1.702×10^{-5}
G	1.329×10^{-5}	6.200×10^{-6}	1–2.407×10^{-5}	4.580×10^{-6}
T	4.360×10^{-6}	7.270×10^{-6}	3.960×10^{-6}	1–1.559×10^{-5}

[a]For example $t_{AC} = 6.550 \times 10^{-6}$.

Table 4: The base mutation matrix t for *Drosophila* (Petrov and Hartl, 1999). Only the relative rates are significant.

	A	C	G	T
A	1–4.0×10^{-5}	1.0×10^{-5}	1.6×10^{-5}	1.4×10^{-5}
C	1.8×10^{-5}	1–6.0×10^{-5}	1.2×10^{-5}	3.0×10^{-5}
G	3.0×10^{-5}	1.2×10^{-5}	1–6.0×10^{-5}	1.8×10^{-5}
T	1.4×10^{-5}	1.6×10^{-5}	1.0×10^{-5}	1–4.0×10^{-5}

Table 5: The base mutation matrix for human, non-immune system B-cell genes (Shen *et al.*, 2000). Only the relative rates are significant. Data were generated from counts of observed mutations by the summing the formula $N_{\text{observed mutations x}\to\text{y}} = N_{\text{clones}} N_{\text{bases}} P(x) P(x \to y|x)$ over all genes examined, and averaging the mutation matrix so obtained over the two donors.

	A	C	G	T
A	1–1.86×10^{-5}	0.0×10^{-5}	1.4×10^{-5}	0.46×10^{-5}
C	2.2×10^{-5}	1–5.73×10^{-5}	0.33×10^{-5}	3.2×10^{-5}
G	5.9×10^{-5}	0.0×10^{-5}	1–7.5×10^{-5}	1.6×10^{-5}
T	0.71×10^{-5}	2.3×10^{-5}	0.71×10^{-5}	1–3.72×10^{-5}

Table 6: The base mutation matrix t for mitochondrial DNA in a nematode (Blouin *et al.*, 1998).

	A	C	G	T
A	1–7.60×10^{-7}	4.00×10^{-8}	6.90×10^{-7}	3.00×10^{-8}
C	2.20×10^{-7}	1–2.41×10^{-6}	1.00×10^{-7}	2.09×10^{-6}
G	3.02×10^{-6}	8.00×10^{-8}	1–3.15×10^{-6}	5.00×10^{-8}
T	3.00×10^{-8}	4.00×10^{-7}	1.00×10^{-8}	1–4.40×10^{-7}

Caption for Cover Figure

Emerging patterns from the inherent structure of the genetic code and non-uniform mutation rates in error prone replication. The relative rate of codon mutation above baseline (blue) is shown by color intensity. Non-baseline synonymous changes are green; conservative, orange; and non-conservative, red. The codons are ordered by AAX, CAX, GAX, TAX, ACX, ...